*Journal of Thermal Analysis and Calorimetry, Vol. 96 (2009) 2, 553–560*

# ZINC(II) AND CADMIUM(II) COMPLEXES WITH *o*-HYDROXYBENZOIC ACID OR *o*-AMINOBENZOIC ACID AND 2-METHYLIMIDAZOLE
## IR spectra, X-ray diffraction studies and thermal analysis

*Maria Olczak-Kobza*[*] *and Agnieszka Mrozek*

Institute of General and Ecological Chemistry, Technical University, 90-924 Łódź, Żeromskiego 116, Poland

Mixed complexes of the type: $Zn(Hsal)_2(2\text{-}MeHim)_2$, $Zn(Han)_2(2\text{-}MeHim)_2$, $Cd(Hsal)_2(2\text{-}MeHim)_2$, $Cd(Han)_2(2\text{-}MeHim)_2$, where $Hsal=OHC_6H_4COO^-$, $Han=NH_2C_6H_4COO^-$, 2-MeHim=2-methylimidazol) have been synthesized and characterized by IR spectroscopic and X-ray diffraction studies. Single-crystal X-ray structure of $Cd(Hsal)_2(2\text{-}MeHim)_2$ has been obtained. Thermal behaviour of the compounds was investigated by thermal analysis (TG, DTG, DTA). A coupled TG-MS system was used to analyse the principal volatile products of complexes. Thermal decomposition pathways have been postulated.

***Keywords:*** *aromatic acid, cadmium(II), heteroligand complexes, 2-methylimidazole, thermal analysis, zinc(II)*

## Introduction

The imidazole group is of great importance in biochemistry. It is present in the metallic centers of the metalloproteins and metalloenzymes. In the active centers of the biomolecules nitrogen N(3) of imidazoles is one of the atoms binding metal. Oxygen of carboxyl or hydroxide groups, or oxygen of water molecules are examples of another coordination atoms in the active centers. The research of the new medicines able to treat heavy poisoning (e.g. Cd) is also connected with investigation of heteroligand complexes. Therefore, complexes containing these groups are suitable models to study different aspects of biological molecules [1–4]. In many biologically important molecules, zinc(II) is bounded to the pyridine nitrogen of imidazoles and to the carboxylate groups [5]. Cadmium is a toxic element, and may compete with Zn(II), Cu(II), Ca(II) and Fe(II) for the active site in important biological molecules [6, 7]. Therefore, complexes of the zinc(II) and cadmium(II) containing such ligands are frequently researched by means of spectroscopic, structural and thermal investigation [8–10] and it seems important to study complexes of these metals and compare their properties.

The present work is a continuation of our studies on the synthesis and properties of zinc(II), cadmium(II) and copper(II) heteroligand complexes with aromatic acids and imidazoles. Previously, the results of investigations of $Zn(Hsal)_2$ [11], $Zn(Han)_2$ [12], $Cd(Hsal)_2$ [13], $Cd(Han)_2$ [14], Cu(sal) [15] and Cd(sal) [16] ($sal=OC_6H_4COO^{2-}$) with imidazole, 4-methylimidazole or 1,2-dimethylimidazole were published. Recently, we have prepared new zinc and cadmium complexes with: aromatic acids and 2-methylimidazole.

## Experimental

### *Materials*

P.a. $Zn(NO_3)_2\cdot 6H_2O$, $Cd(NO_3)_2\cdot 4H_2O$, ethanol, toluene (POCH-Gliwice), *o*-hydroxybenzoic acid, *o*-aminobenzoic acid (Fluka Chemie AG), 2-methylimidazole (Aldrich) were used without additional purification.

### Preparation

$Zn(Hsal)_2\cdot 2H_2O$, $Cd(Hsal)_2\cdot 2H_2O$, $Zn(Han)_2$ and $Cd(Han)_2$ were obtained according to the method described in literature [17, 18]. The aqueous solutions of the $Zn(NO_3)_2\cdot 6H_2O$ or $Cd(NO_3)_2\cdot 4H_2O$ were added to a solution of sodium *o*-hydroxybenzoate or sodium *o*-aminobenzoate. The precipitate was washed with several portions of distilled water and ethanol and afterwards dried at room temperature.

$Zn(Hsal)_2(2\text{-}MeHim)_2$, $Cd(Hsal)_2(2\text{-}MeHim)_2$. A mixture of $Zn(Hsal)_2$ or $Cd(Hsal)_2$ and 2-methylimidazole in ethanol was heated to 333 K and stirred. The mixture was allowed to reflux for 3 h, the hot solution was filtered, and left to crystallize. The resulting white precipitates were washed with ethanol and dried in air. The mixed complexes obtained when the molar ratio of the reagents was kept at the level of 1:3.

---

[*] Author for correspondence: bpacewska@pw.plock.pl

*1388–6150/$20.00*

*Akadémiai Kiadó, Budapest, Hungary*
*Springer, Dordrecht, The Netherlands*

Single crystals suitable for X-ray diffraction studies were obtained only for Cd(Hsal)$_2$(2-MeHim)$_2$ by slow evaporation of the ethanol solution.

Zn(Han)$_2$(2-MeHim)$_2$, Cd(Han)$_2$(2-MeHim)$_2$. Syntheses were carried out in two-phase system consisting of solid zinc or cadmium di(*o*-aminobenzoate) and toluene solution of 2-methylimidazole. The mixture was heated to 333 K and stirred for 14 h and then the hot mixture was filtered. The white precipitates were washed with acetone and dried in air. The reactions were carried out at molar ratio 1:2.

### *Methods*

#### Chemical analysis

The zinc(II) and cadmium(II) were determined by complexometric titration with disodium ethylenediaminotetraacetate (EDTA) [19], while carbon, hydrogen and nitrogen – by elemental analysis using Euro Vector, Euro EA analyser.

#### X-ray analysis (XRD)

The X-ray analysis was carried out by means of a Siemens D 5000 powder diffractometer, using CuK$_\alpha$ radiation, 2Θ range 2–80°. The products of synthesis and the products of decomposition were studied using X-ray powder method.

Colourless crystals, suitable for X-ray experiment, were obtained only for Cd(Hsal)$_2$(2-MeHim)$_2$. All measurements of the crystals were performed on Kuma 4-CCD *k*-axis diffractometer with graphite-monochromated MoK$_\alpha$ radiation at room temperature. The crystals were positioned at 62 mm from the KM4-CCD camera, 496 frames were measured at 1.5 intervals with a counting time of 25 s. The data were corrected for Lorentz and polarization effects. Multi-scan absorption correction was applied. Data reduction and analysis were carried out with the Kuma Diffraction (Wrocław) programs [20].

The structures were solved by direct methods [21] and refined using SHELXL 93 [22]. The full-matrix least-squares refinement was based on $F^2$ and applied nisotropic temperature factors for all non-H-atoms; positions of all H-atoms were found from electron density maps and were refined in raiding model with the isotropic displacement parameters of 1.5 times the respective U$_{eq}$ values for the parent atoms. Atomic scattering factors were obtained from SHELXL [22].

#### Infrared (IR) analysis

IR spectra were recorded using a Zeiss Specord M80 spectrophotometer in the range of 400–4000 cm$^{-1}$. The samples were prepared in the form of KBr pellets.

#### Thermal studies

The thermoanalytical measurements were carried out using a Balzers TG/DTA-SETSYS-16/18 thermoanalyzer connected with Thermostar (Balzers) mass spectrometer. The temperature range 293–1273 K; the heating rate β=10 K min$^{-1}$, in air atmosphere; the sample mass – a dozen or so milligrams weighed in corundum crucible. A coupled TG-MS system was used to analysis of principal species evolved during the dynamic thermal decomposition of fragmentation processes of all complexes: flow rate 1 L h$^{-1}$.

## Results and discussion

### *Formulae, X-ray and spectroscopy properties of the complexes*

The four new complexes were obtained. The results of the chemical analysis and formulae of these compounds are presented in Table 1. The XRD powder analysis was necessary in order to define the purity of the final products. This analysis showed additionally that the all heteroligand complexes have crystalline structures (Fig. 1).

IR spectroscopic investigation was conducted in order to define the zinc(II) and cadmium(II) atoms surrounding in the complexes. The positions of the

**Table 1** Results of chemical analysis

| Compound | Molecular formula | $M$/%* | | C/% | | H/% | | N/% | |
|---|---|---|---|---|---|---|---|---|---|
| | | calc. | found | calc. | found | calc. | found | calc. | found |
| Zn(Hsal)$_2$(2-MeHim)$_2$ | Zn(C$_7$H$_5$O$_3$)$_2$(C$_4$H$_6$N$_2$)$_2$ | 12.99 | 12.4 | 52.49 | 52.7 | 4.41 | 4.8 | 10.57 | 11.1 |
| Cd(Hsal)$_2$(2-MeHim)$_2$ | Cd(C$_7$H$_5$O$_3$)$_2$(C$_4$H$_6$N$_2$)$_2$ | 20.42 | 20.3 | 47.96 | 47.9 | 4.00 | 4.0 | 10.17 | 10.4 |
| Zn(Han)$_2$(2-MeHim)$_2$ | Cd(C$_7$H$_6$NO$_2$)$_2$(C$_4$H$_6$N$_2$)$_2$ | 13.04 | 13.1 | 52.63 | 52.1 | 4.78 | 4.9 | 16.74 | 16.8 |
| Cd(Han)$_2$(2-MeHim)$_2$ | Cd(C$_7$H$_6$NO$_2$)$_2$(C$_4$H$_6$N$_2$)$_2$ | 20.49 | 20.1 | 48.12 | 47.9 | 4.37 | 4.5 | 15.31 | 15.7 |
| Zn(2-Meim)$_2$* | Zn(C$_4$H$_5$N$_2$)$_2$ | – | – | 42.22 | 43.8 | 4.40 | 4.3 | 24.64 | 19.9 |

*the intermediate product of reaction: (1), (3)

**Table 2** Valency and bending vibrations bands of $COO^-$ , $COH^-$ and NH groups ($cm^{-1}$)

| Complex | $\nu_{as(COO^-)}$ | $\nu_{s(COO^-)}$ | $\Delta\nu$ | $\nu_{COH}$ | $\delta_{COH}$ | $\nu_{NH}$ |
|---|---|---|---|---|---|---|
| Na(Hsal) | 1581s | 1385s | 196 | 1248s | 1317w | – |
| $Zn(Hsal)_2$ | 1530m | 1384s | 146 | 1243s | 1324m | – |
| $Cd(Hsal)_2$ | 1575m | 1385s | 190 | 1252s | 1348m | – |
| $Zn(Hsal)_2(2\text{-}MeHim)_2$ | 1568s | 1393s | 175 | 1256s | 1348m | 3234m |
| $Cd(Hsal)_2(2\text{-}MeHim)_3$ | 1572m | 1383s, 1392s | 189, 180 | 1245s | 1348m | 3254m |

s – strong, m – middle, w – weak

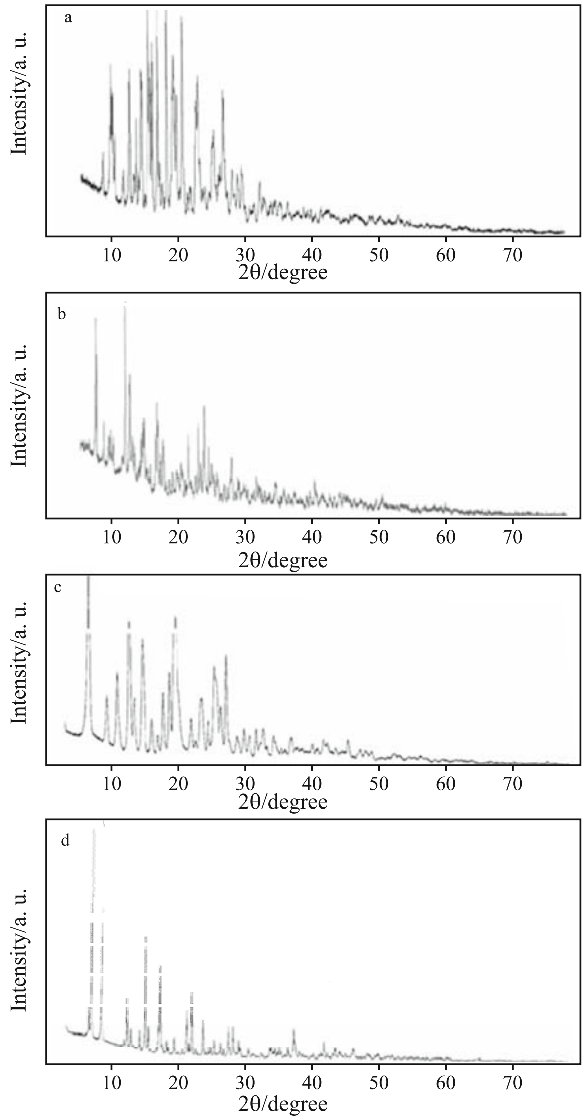

**Fig. 1** X-ray diffraction patterns of complexes:
a – $Zn(Hsal)_2(2\text{-}MeHim)_2$, b – $Cd(Hsal)_2(2\text{-}MeHim)_2$,
c – $Zn(Han)_2(2\text{-}MeHim)_2$, d – $Cd(Han)_2(2\text{-}MeHim)_2$

bands connected with vibrations of the carboxylate, phenyl, amine, and imine groups were analysed in the range of 1600–1300 and 3500–3100 $cm^{-1}$. In the spectrum of all the complexes, the splitting $\Delta\nu$ ($\Delta\nu=\nu_{as(COO^-)}-\nu_{s(COO^-)}$) were compared with $\Delta\nu$ of the sodium salts. The splitting $\Delta\nu$ in the complexes with *o*-hydroxybenzoic acid is smaller than that for the sodium salt in which this group is monodentate (Table 2). Due to spectroscopic criterion [23], the bidentate carboxylate groups exist in the prepared complexes. The phenyl group of *o*-hydroxybenzoate ion is free because the intense bands of the stretching vibrations $\nu_{COH}$ appear near 1248 $cm^{-1}$ (1256 and 1245 $cm^{-1}$, respectively) and bending vibrations $\delta_{COH}$ are detectable for all the compounds [24–26]. In the compounds with the bonding of the phenol group, band $\delta_{COH}$ is absent [24] and band $\nu_{COH}$ is shifted to lower frequencies [25].

The unassociated NH group of free molecules of imidazoles gives a $\nu_{NH}$ band at 3500 $cm^{-1}$ and $\delta_{NH}$ band near 1450 $cm^{-1}$. In compounds with metals, $\nu_{NH}$ bands (one or two) are shifted towards lower frequencies and the $\delta_{NH}$ is often invisible or appears within the range 1400–1450 $cm^{-1}$ [27, 28]. Just the same modifications are observed in the present's complexes. In the spectrum of the zinc(II) and cadmium(II) complexes $\nu_{NH}$ band is observed at 3245 and 3254 $cm^{-1}$, respectively and the band $\delta_{NH}$ is invisible (Table 2).

The splitting $\Delta\nu$ in the complexes with *o*-aminobenzoic acid is different. In the complex of zinc(II) it is higher than that for the sodium salt, in the complex of cadmium(II) it is smaller. Due to spectroscopic criterion, the monodentate carboxylate groups exist in the zinc complex and the bidentate in the cadmium one. The amine groups do not form bonds in heteroligand compounds because the bands $\nu_{as(NH_2)}$ and $\nu_{s(NH_2)}$ appear near that for the sodium salt (Table 3). When the amine groups form the bonds, $\nu_{as(NH_2)}$ and $\nu_{s(NH_2)}$ are shifted to lower frequencies. The band $\nu_{NH}$ of 2-methylimidazole is shifted towards lower frequencies and $\delta_{NH}$ is invisible analogous how in the complexes of *o*-hydroxybenzoic acid (Table 3).

## Structure of $Cd(Hsal)_2(2\text{-}MeHim)_2$

X-ray structure analysis of $Cd(Hsal)_2(2\text{-}MeHim)_2$ was conducted. Figure 2 shows the molecular unit of the compound. All details of X-ray structure analysis are summarized in Table 4 and selected geometrical parameters are gathered in Table 5. The metal ion is in

**Table 3** Valency and bending vibrations bands of $COO^{-}$, $NH_2$ and NH groups ($cm^{-1}$)

| Complex | $\nu_{as(COO^-)}$ | $\nu_{s(COO^-)}$ | $\Delta\nu$ | $\nu_{as(NH_2)}$ | $\nu_{s(NH_2)}$ | $\nu_{NH}$ |
|---|---|---|---|---|---|---|
| Na(Han) | 1532s | 1392s | 140 | 3440s, 3408m | 3328s | – |
| $Zn(Han)_2$ | 1536s,1546m | 1408s | 128,138 | 3300s, 3260sh | 3140s | – |
| $Cd(Han)_2$ | 1535s | 1402s | 133 | 3292s, 3250sh | 3140s | – |
| $Zn(Han)_2(2\text{-}MeHim)_2$ | 1541s | 1375s | 166 | 3461m, 3441m | 3335m | 3298m |
| $Cd(Han)_2(2\text{-}MeHim)_2$ | 1518s | 1387s | 131 | 3460m, 3414m | 3346m | 3310w |

s – strong, m – middle, w – weak, sh – shoulder

**Table 4** Crystal data and summary of intensity data collection and structure refinement for $Cd(Hsal)_2(2\text{-}MeHim)_2$

| Empirical formula | $CdC_{22}N_4O_6H_{22}$ |
|---|---|
| Formula mass | 550.85 |
| Temperature/K | 293 |
| Wavelength/Å | 0.71073 |
| Crystal system | Triclinic |
| Space group | P-1 |
| *a*/Å | 8.0200(4) |
| *b*/Å | 11.6159(6) |
| *c*/Å | 13.5304(7) |
| α/° | 89.101(4) |
| β/° | 79.572(4) |
| γ/° | 75.566(4) |
| Volume/$Å^3$ | 1199.96(11) |
| *Z* | 2 |
| Calculated density/Mg $m^{-3}$ | 1.525 |
| Absorption coefficient | 0.953 |
| *F*(000) | 556 |
| θ range/° | 3.31 to 25 |
| Index ranges | $-8<h<9$<br>$-13<k<13$<br>$-16<l<16$ |
| Reflections collected/unique | 9834/4214 |
| Refinement method | $F^2$ |
| Data/restrains/parameters | 4214/0/308 |
| Goodnes-of-fit on $F^2$ | 1.035 |
| $R_1$ indices [$I>2\sigma(I)$] | 0.0383 |
| $wR_2$ | 0.0552 |
| Largest difference peak and hole/e $Å^{-3}$ | 0.33 and –0.37 |

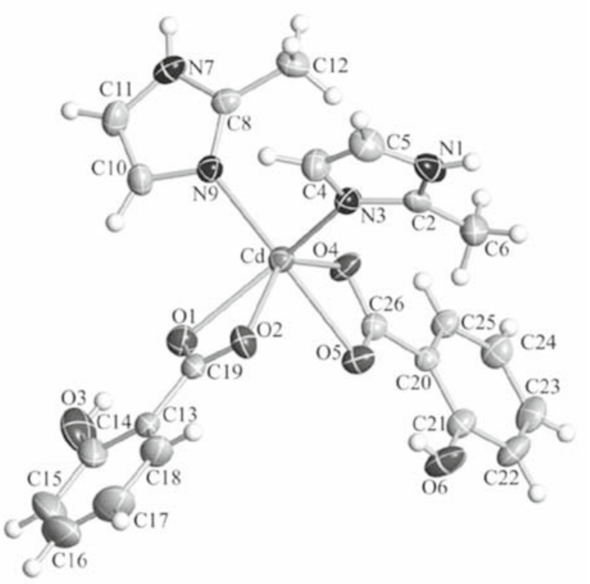

**Fig. 2** Molecular structure of $Cd(Hsal)_2(2\text{-}MeHim)_2$ complex

distorted *cis*-octahedral coordination involving two unidentate heterocyclic N-bound imidazole molecules and two O,O bidentate carboxylate groups in the $CdO_4N_2$ polyhedron, three oxygen atoms (O1, O2 and O4) and a nitrogen atom (N3) constitute the basal plane, with an r.m.s. deviation of 0.385(1) Å. The Cd atom is 0.411(1) Å above the plane towards atom N9. Atoms N9 and O5 are located at the two axial position of the octahedron. The angle O5–Cd–N9 equals 146.67(7)° and all other angles around the central Cd atom deviate significantly from 90°, indicating a severely distorted octahedral geometry (Table 5). Hence, for full octahedron description, the two Cd–N and four Cd–O distances are essential. The Cd–N3 and Cd–N9 distances of 2.236(2) and 2.244(2) Å, respectively are typical within imidazole-type ligands [29]. For 5 structurally similar Cd(II) complexes found in Cambridge Crystallographic Database (CSD, version 1.9 of May 2007) [30] the average value of Cd–N distance is 2.278 Å. The distances between cadmium and oxygen atoms are about 0.15 Å longer than Cd–N ones what is typical for such kind of compounds. What's more the bond distances of bidentate ligands are visibly asymmetric. To confirm this conclusion we performed searching of the CSD, which gave us 113 structures of $Cd(bidentate)_2(unidentate)_2$ type. In all found compounds the bonds connecting bidentate ligands and Cd atom are also asymmetric and the difference in bond lengths is about 0.1 Å.

In salicylic acid molecules both carboxylic oxygen atoms are involved in H-bonds network, however

**Table 5** Selected geometric parameters (Å,°) and hydrogen-bonding geometry (Å,°) for $Cd(Hsal)_2(2\text{-}MeHim)_2$

| | | | |
|---|---|---|---|
| Cd–O1 | 2.391(2) | Cd–O5 | 2.452(2) |
| Cd–O2 | 2.405(2) | Cd–N3 | 2.236(2) |
| Cd–O4 | 2.346(2) | Cd–N9 | 2.244(2) |
| | | | |
| O5–Cd–N9 | 146.67(7) | O5–Cd–N3 | 103.65(7) |
| O2–Cd–O4 | 136.37(6) | O5–Cd–O1 | 87.39(6) |
| O2–Cd–N3 | 89.56(7) | N9–Cd–N3 | 99.01(8) |
| O1–Cd –N3 | 141.31(7) | N9–Cd–O2 | 121.12(7) |
| O1–Cd–O4 | 107.58(6) | N9–Cd–O4 | 95.34(7) |
| O5–Cd–O2 | 83.45(6) | N9–Cd–O1 | 90.01(7) |
| O5–Cd–O4 | 54.30(6) | | |

| D–H...A | D–H | H…A | D…A | D–H…A | Symmetry code |
|---|---|---|---|---|---|
| O3–H3...O1 | 0.73 | 1.94 | 2.571(4) | 145 | |
| O6–H6...O5 | 0.70 | 1.91 | 2.563(3) | 154 | |
| N1–H1...O2 | 0.86 | 2.07 | 2.851(3) | 150 | –x, 2–y, 1–z |
| N7–H7...O4 | 0.86 | 1.97 | 2.785(3) | 157 | –x, 2–y, –z |

O1 and O5 create intramolecular bonds to oxygen atoms from hydroxyl groups while O2 and O4 atoms are connected via H1 to N1 and via H7 to N7 nitrogens from imidazole moieties respectively. Intermolecular H-bonds create 12-membered rings involving two cadmium atoms, two salicylate oxygens and two imidazole moieties. Connected molecules build polymeric chain along *z*-axis. Geometrical parameters for H-bonding are collected in Table 5.

*Thermal analysis*

Figure 3 presents TG, DTG and DTA curves of the complexes, and Table 6 presents the temperature range, mass loss and nature of the peaks in each stage of the decomposition. The successive solid products of decomposition were obtained at temperatures determined on the basis of the TG curves. XRD and chemical analyses of these products were carried out.

Diffraction patterns were compared to PDF ICSD36-1451 in order to identify inorganic cadmium compounds. A coupled TG-MS system was used to study of gaseous species evolved during dynamic thermal decomposition (or fragmentation) process. Ionic current intensities were noted with sensitivity between E 9–E 13.

$Zn(Hsal)_2(2\text{-}MeHim)_2$

The decomposition of the $Zn(Hsal)_2(2\text{-}MeHim)_2$ complex begins with the phase transition (endothermic peak in DTA curve at 403 K). The fused samples decompose in two stages. The first step begins at 433 K. Significant mass loss (58.2%) and intense

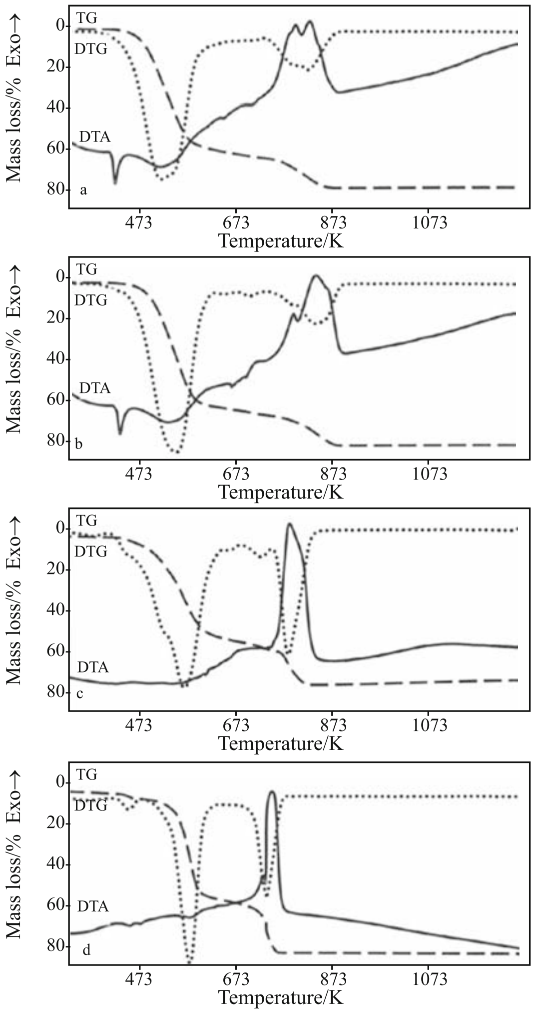

**Fig. 3** Thermal curves of complexes:
a – $Zn(Hsal)_2(2\text{-}MeHim)_2$, b – $Cd(Hsal)_2(2\text{-}MeHim)_2$,
c – $Zn(Han)_2(2\text{-}MeHim)_2$, d – $Cd(Han)_2(2\text{-}MeHim)_2$

**Table 6** Results of thermal analysis

| Complex | Stage | Temperature range/K | Formulae | Mass loss/% |  | Peak nature | Temperature/ K |
|---|---|---|---|---|---|---|---|
|  |  |  |  | calc. | found |  |  |
| $Zn(Hsal)_2(2\text{-}MeHim)_2$ | I | 433–603 | Zn(2-Meim) | 54.80 | 58.2 | endo | 528 |
|  | II | 643–866 | ZnO | 83.84 | 85.0 | exo | 783 |
| $Cd(Hsal)_2(2\text{-}MeHim)_2$ | I | 443–585 | CdO+org.fragm. | 50.12 | 48.9 | endo | 453, 518 |
|  | II | 603–793 | CdO | 76.68 | 77.8 | exo | 718, 758 |
| $Zn(Han)_2(2\text{-}MeHim)_2$ | I | 443–603 | Zn(2-Meim) | 54.27 | 52.5 | endo | 443, 533 |
|  | II | 603–868 | ZnO | 83.77 | 86.2 | exo | 768, 822 |
| $Cd(Han)_2(2\text{-}MeHim)_2$ | I | 423–623 | CdO+org.fragm. | 49.94 | 51.0 | endo | 503, 553 |
|  | II | 633–798 | CdO | 76.60 | 82.0 | exo | 703, 713, 778 |

peak are observed in the TG and DTG (528 K) curves. A small and broad endothermic peak in the DTA was found at 528 K. In the second stage mass loss is 85.3%. In the DTG curve is observed peak at 778 K and in DTA big peak exo at 783 K (Fig. 3a, Table 6). The mass loss and elemental analysis indicated that in the first stage forms $Zn(2\text{-}Meim)_2$ and the X-ray powder analysis showed that intermediate product is amorphous (Table 1, Fig. 4a). The oxide ZnO forms in the second stage.

The signals of ionic current are observed in the ranges 493–623 and 733–833 K. The signals from release ions with *m*/*z*=44, 45, 46 appear in the first range and with *m*/*z*=15, 30, 44, 45, 46, 78 (trace) in the second one. These values *m*/*z* are assigned to the ions: $CO_2^+$, $^{13}C^{16}O_2^+$, $^{12}C^{18}O^{16}O^+$ and $CH_3^+$, $NO^+$, $CO_2^+$, $^{13}C^{16}O_2^+$, $^{12}C^{18}O^{16}O^+$, $C_6H_6^+$. Moreover ionic current signals with *m*/*z*=50, 51, 52 and 77 were mentioned in the course of decomposition and they were attributed to fragments coming from basic molecular ions. The ionic current signal from release of $CH_3^+$ (*m*/*z*=15) does not increase till the second stage and the pathway of decomposition proceeds in accordance with reaction Scheme (1):

$$Zn(Hsal)_2(2\text{-}MeHim)_2 \rightarrow Zn(2\text{-}Meim)_2 \rightarrow ZnO \quad (1)$$

where 2-Meim – $C_4N_2H_5$.

### $Cd(Hsal)_2(2\text{-}MeHim)_2$

The decomposition of the $Cd(Hsal)_2(2\text{-}MeHim)_2$ starts in the solid-state (443 K in the TG curve) and then the phase transition occurs (peak endo 453 in DTA). The fused sample decomposes in two stages. The big mass loss (TG) and intense peak (DTG) are observed in the first stage. This stage is endothermic (the next peak 518 K in DTA). The second stage is folded. In the DTG curves there are two peaks at 698, 758 K and in the DTA two exothermic peaks at 718 and 758 K (Fig. 3b, Table 6). The mass loss and elemental analysis indicated that the intermediate product has formulae $Cd(2\text{-}Meim)_2$ but XRD analysis showed that this product is a mixture CdO and different solid organic fragments (Fig. 4b). In the second stage forms pure CdO. The gaseous products of decomposition are observed in the broad range of the temperature 503–873 K. The signals of ionic current intensities of $CO_2^+$, $^{13}C^{16}O_2^+$ and $^{12}C^{18}O^{16}O^+$ (*m*/*z*=44, 45, 46, respectively) have centers at 553, 793 K. The ion signal intensities of $NO^+$ (*m*/*z*=30) have centers at 773 and 853 K. Moreover ionic current signals with *m*/*z*=22, 52 were mentioned and they were attributed to fragments coming from basic molecular ions. Thermal decomposition proceeds in accordance with reaction Scheme (2):

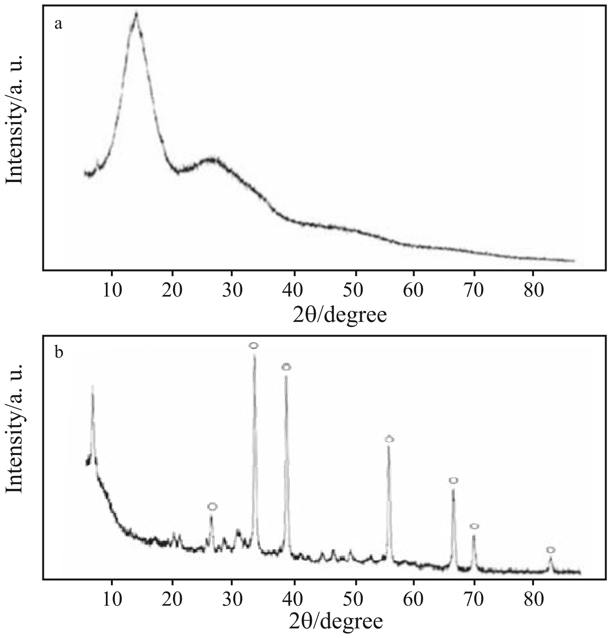

**Fig. 4** X-ray diffraction patterns of the intermediate products: a – $Zn(2\text{-}Meim)_2$, b – CdO (°) and solid organic fragments

$$Cd(Hsal)_2(2\text{-}MeHim)_2 \rightarrow CdO\text{+org. fragm.} \rightarrow CdO \quad (2)$$

### $Zn(Han)_2(2\text{-}MeHim)_2$

The decomposition of the $Zn(Han)_2(2\text{-}MeHim)_2$, occurs in two stages. The decomposition begins at 443 K together with fused sample. The big mass loss and broad peak are observed in the TG and DTG (533 K) curves. DTA curve shows the sharp, endothermic peak at 443 K and small lowering near 533 K in the further course of the curve. The second stage is a folded. The peaks at 768 and 822 K are observed in the DTG, and two intensive, exothermic peaks are found in DTA curve at the same temperature (Fig. 3c, Table 6). The mass loss, and elemental analysis indicate that in the first stage forms $Zn(2\text{-}Meim)_2$ (Tables 1 and 6), pure oxide ZnO forms in the second one. X-ray powder diffraction patterns products of decomposition are analogous as in the case of decomposition of the $Zn(Hsal)_2(2\text{-}MeHim)_2$.

The mass spectra of the $Zn(Han)_2(2\text{-}MeHim)_2$ presents signals of ionic current in the ranges 453–603 and 693–903 K. In the first range appear the ionic current signals from release ions with *m*/*z*=44, 45, 46 ($CO_2^+$, $^{13}C^{16}O_2^+$, $^{12}C^{18}O^{16}O^+$). In the secon one appear the signals with *m*/*z*=15, 30, 44, 45, 46, 78 ($CH_3^+$, $NO^+$, $CO_2^+$, $^{13}C^{16}O_2^+$, $^{12}C^{18}O^{16}O^+$, $C_6H_6$ (trace)). Moreover ionic current signals with *m*/*z*=50, 51, 52 were mentioned and they were attributed to fragments coming from basic molecular ions. The reaction scheme of decomposition is following:

$$Zn(Han)_2(2\text{-}MeHim)_2 \rightarrow Zn(2\text{-}Meim)_2 \rightarrow ZnO \quad (3)$$

### $Cd(Han)_2(2\text{-}MeHim)_2$

The decomposition of $Cd(Han)_2(2\text{-}MeHim)_2$ complex starts at 448 K and the first stage is described by peak at 558 K in DTG curve. The small peak at 503 K and lowering near 553 K are observed in DTA curve (Fig. 3d, Table 6). The mass loss of the second stage begins at 633 K. This stage is folded. Peaks at 698, 773 K found in the DTG and three peaks at 703, 713, 778 K in DTA. The mass loss and chemical analysis indicated that the intermediate products have formulae $Cd(2\text{-}Meim)_2$ but the XRD analysis showed that this product is a mixture CdO and solid organic fragments analogous as in the case of the decomposition of the $Cd(Hsal)_2(2\text{-}MeHim)_2$. Pure CdO is the final product of decomposition. The signals of ionic current of the gaseous products of decomposition of the $Cd(Hsal)_2(2\text{-}MeHim)_2$ are observed in the broad range of the temperature for ions: $CO_2^+$, $^{13}C^{16}O_2^+$, $^{12}C^{18}O^{16}O^+$ (513–833 K), with maximum at 573, 693, 763 K. The ionic current signal from release ion $NO^+$ (*m*/*z*=30) appears in the second range of decomposition. Moreover ionic current signals with *m*/*z*=51, 52, 77 were mentioned and they were attributed to fragments coming from basic molecular ions. The pathway of decomposition proceeds in accordance with reaction Scheme (4)

$$Cd(Han)_2(2\text{-}MeHim)_2 \rightarrow CdO\text{+org. fragm.} \rightarrow CdO \quad (4)$$

## Conclusions

The heteroligand complexes were obtained at the molar ratio of the $M(H_2sal)_2$ to 2-methylimidazole 1:3 and $M(H_2an)_2$ to 2-methylimidazole 1:2 (where *M*= Zn, Cd). When the molar ratio was greater than 1:3, the mixture of the complex and 2-methylimidazole was obtained. All the new complexes have a crystalline structure.

The spectroscopic (IR) investigation and X-ray structure analysis of $Cd(Hsal)_2(2\text{-}MeHim)_2$ gave the information about surrounding of metals in these compounds. The *o*-hydroxybenzoate ion is bidentate either in homoligand or in heteroligand complexes. In investigated complexes metal forms bonds with bidentate group $COO^-$ and with nitrogen N(3) of 2-methylimidazole.

The *o*-aminobenzoate ion is tridentate in homoligand complexes $M(Han)_2$, however, it is monodentate in heteroligand compound of zinc and bidentate in analogous compound of cadmium. Zinc forms bonds with monodentate $COO^-$ group and with nitrogen N(3) of 2-methylimidazole, cadmium is connected to bidentate $COO^-$ group and to nitrogen N(3) of 2-methylimidazole. In the $Cd(Hsal)_2(2\text{-}MeHim)_2$ complex cadmium analogous how in the many compound of $Cd(bidentate)_2(unidentate)_2$ type forms two asymmetric bonds with bidentate $COO^-$ group and distance Cd–O are longer than Cd–N [12, 29].

The thermal decomposition of the complexes is two-stage process but the pathway of decomposition is different for compounds of zinc or cadmium. The intermediate product is $Zn(2\text{-}Meim)_2$ in the case of zinc compounds, but CdO and solid organic fragments in the case of cadmium compounds. Metal oxide and gaseous products are final products. The mass spectra of all the complexes presents the similar signals. The principal ion intensities correspond to: $NO^+$, $CO_2^+$ as well as $^{13}C^{16}O_2^+$ and $^{12}C^{18}O^{16}O^+$ (*m*/*z*=30, 44, as well as 45, 46, respectively). In the case of complexes of zinc the ionic current signals from release of $CH_3^+$ and $C_6H_6^+$ (*m*/*z*=15, 78) were observed additional. Therefore, the different ways of zinc and cadmium complexes decomposition should be taken under consideration.

The thermal stability, described by $T_i$, decreases in the following order:

$$\begin{array}{ccc} Zn(Han)_2(2\text{-}MeHim)_2 & = & Cd(Hsal)_2(2\text{-}MeHim)_2 > \\ 443\text{ K} & & 443\text{ K} \\ Zn(Hsal)_2(2\text{-}MeHim)_2 & > & Cd(Han)_2(2\text{-}MeHim)_2 \\ 433\text{ K} & & 423\text{ K} \end{array}$$

and it is lower than the stability of homoligand complexes: $M(H_2sal)_2$ ($T_{iZn}$=513 K, $T_{iCd}$=503 K) and $M(H_2an)_2$ ($T_{iZn}=T_{iCd}$ =673 K). ($T_i$ – the temperature at which the rate of decomposition is visible).

## References

1 N. M. Sivasankarani, S. Jawaharunnissa and L. Kamakskil, Ind. J. Chem., 29A (1990) 581.
2 A. Busnot, F. Busnot, J. F. Hemidy and J. F. Le Querler, Thermochim. Acta, 228 (1993) 219.
3 D. Czakis-Sulikowska, J. Radwańska-Doczekalska, A. Czylkowska, M. Markiewicz and A. Broniarczyk, J. Therm. Anal. Cal., 86 (2006) 327.
4 O. Z. Yesile, H. Ölmez and H. Icbudok, J. Therm. Anal. Cal., 89 (2007) 555.
5 R. J. Sundberg and R. B. Martin, Chem. Rev., 74 (1974) 473.
6 W. Seńczuk, Toksykologia, PZWL, Warsaw 1994.
7 J. Brandys, Toksykologia – wybrane zagadnienia, Wydawnictwo UJ, Cracow 1999.
8 N. M. Sivasankarani, S. Jawaharunnissa and L. Kamakskil, Ind. J. Chem., 29A (1990) 581.
9 Patel, R. P. Srivastawa, N. Singh, S. Kumar and K. B. Pandeja, Ind. J. Chem., 40A (2001) 361.
10 A. Busnot, F. Busnot, J. F. Hemidy and J. F. Le Querler, Thermochim. Acta, 228 (1993) 219.
11 M. Olczak-Kobza, R. Czylkowski and J. Karolak-Wojciechowska, J. Therm. Anal. Cal., 74 (2003) 895.
12 M. Olczak-Kobza, Thermochim. Acta, 419 (2004) 67.
13 M.Olczak-Kobza, A. Dzierżawska-Majewska and J. Karolak-Wojciechowska, J. Coord. Chem., 59 (2006) 545.
14 M. Olczak-Kobza, J. Anal. Appl. Pyrolysis, 78 (2007) 400.
15 A. Turek and M. Olczak-Kobza, J. Therm. Anal. Cal., 54 (1998) 133.
16 M. Olczak-Kobza, Thermochim. Acta, 366 (2001) 129.
17 K. Rissanen, J. Valkonen, P. Kokkonen and M. Lsskala, Acta Chem. Scand., A41 (1987) 299.
18 G. Hill and C. Curren, J. Phys. Chem., 64 (1960) 1519.
19 A. Cygański, Chemiczne metody analizy ilościowej, WNT, Warsaw 1999, p. 526.
20 UNIL IC & KUMA (2000), CrysAlis CCD. Version 1.163; Kuma Diffraction Instruments GmbH, Wrocław, Poland.
21 G. M. Sheldrick, SHELXTL PC$^{MT}$, Siemens Analytical X-Ray Instruments Inc., Madison, Wisconsin, USA 1990.
22 G. M Sheldrick, SHELXL-93.A FORTRAN-77 Program for the Refinement of Crystal Structures from Diffraction Data. University of Göttingen, Germany 1993.
23 C. B. Beacon and R. J. Philips, Coord. Chem. Rev., 33 (1980) 227.
24 K. Rissanen, J. Valkonen, P. Kokkonen and M. Lsskala, Acta Chem. Scand., A41 (1987) 299.
25 J. A. Haritonow and E. K. Tujebahow, Koord. Khim., 10 (1984) 376.
26 L. Abuhijleh and C. Woods, Inorg. Chem. Commun., 4 (2001) 119.
27 W. J. Eilbeck, F. Holmes and A. E. Underhill, J. Chem. Soc., A (1967) 757.
28 W. J. Eilbeck, F. Holmes, Ch. E. Taylor and A. E. Underhill, J. Chem. Soc., A (1968) 128.
29 S. J. Lippard, Progr. Inorg. Chem., 23 (1977) 1.
30 F. H. Allen, Acta Cryst., B58 (2002) 380.

Received: February 4, 2008
Accepted: April 16, 2008
Online First: April 13, 2009

DOI: 10.1007/s10973-008-9048-5